

EPR and Optical Absorption Studies of Cu²⁺ in Boro-Arsenate Glasses

M. Purnima^a, Avula Edukondalu^{a,b,*}, K. Siva Kumar^{a,b}, Syed Rahman^a

^a Department of Physics, Osmania University, Hyderabad, Telangana, India

^b Department of Physics, University College for Women, Koti, Hyderabad, Telangana, India

Received: January 20, 2016; Revised: June 6, 2016; Accepted: November 3, 2016

Electron paramagnetic resonance (EPR) and optical absorption studies of xMgO-(25-x)Li₂O-50B₂O₃-25As₂O₃ glasses were made by introducing Cu²⁺ as a spin probe. The EPR spectra of all the glass samples recorded at X-band frequencies have similar spectral features. The Cu²⁺ ions are in well-defined axial sites, but subjected to small distortion leading to the broadening of the spectra. The spin-Hamiltonian parameter values indicate that the ground state of Cu²⁺ is $d_{x^2-y^2}$ and the site symmetry around Cu²⁺ ions is tetragonal distorted octahedral. The optical absorption spectra exhibited a broadband corresponding to the d-d transition bands of Cu²⁺ ion. By correlating EPR and optical data, the bond parameters were evaluated and the values show purely ionic nature for the in-plane σ bonding and in-plane π bonding. The out-of-plane π bonding is moderately covalent.

Keywords: Glass, spin-Hamiltonian, Optical Absorption, Electron Spin Resonance

1. Introduction

Heavy metal oxide based glasses containing As₂O₃ has received significant attention owing to their interesting optical applications. These glasses have large non-linear optical susceptibility coefficient¹⁻⁴ that makes them suitable for potential applications in non-linear optical devices (such as ultra-fast optical switches and power limiters), broad band optical amplifiers operating around 1.5 μm and in a number of solid state ionic devices.

Electron paramagnetic resonance (EPR) spectroscopy is an experimental technique sometimes capable of determining the co-ordination and environment of paramagnetic ions in glasses^{5,6}. EPR behaviors of oxide glasses doped with transition metal (TM) ions have been extensively studied to obtain information on the glassy network and to identify the site symmetry around the TM ions⁷⁻¹⁰. Glasses containing TM ions exhibit memory and photo conducting properties¹¹. Recently, Sumalatha et al.¹², Hayder Khudhair Obayes et al.¹³, Edukondalu et al.¹⁴ studied the local structure around Cu²⁺ ion in oxide glasses by EPR spectra. Copper (II) is the most amenable ion for EPR studies. The main advantage of using Cu²⁺ as the spin probe is that its EPR spectra can easily be recorded at room temperature, the spectrum is simple and the spread of the spectrum is large enough to detect minute changes in the coordination sphere¹⁵.

Optical absorption of transition metal ions in glasses is influenced by the host structure into which the transition metal ions are incorporated. In oxide glasses, the TM ions mostly form coordination complexes with doubly charged oxygen as the ligands. The actual structure will depend on the composition of the glass system¹⁶. By correlating the EPR

and optical spectra, one can obtain information regarding the bond parameters which determine the metal-ligand bond in the glasses. The properties of a glass can often be altered by the addition of a network modifier to the basic constituents. The commonly used network modifiers are the alkali and alkaline earth oxides¹⁷. It was observed that the properties of an alkali oxide glass show a non-linear behavior when one kind of alkali is gradually replaced by another. This departure from linearity is called the mixed alkali effect¹⁸. Similar observations were made in the case of mixed alkali-alkaline earth oxide glasses¹⁹. This phenomenon is called mixed oxide effect. In this paper, we report EPR and optical absorption studies of Cu²⁺ spin probe in the quaternary glass system xMgO-(25-x)Li₂O-50B₂O₃-25As₂O₃. The influence of varying the concentrations of Li₂O and MgO, which acts as network modifiers on the spin-Hamiltonian parameters, is discussed.

2. Experimental

Pure and copper (1 mole %) doped glass, samples of composition (table 1) xMgO-(25-x)Li₂O-50B₂O₃-25As₂O₃ (0 ≤ x ≤ 25) were prepared using the conventional melt-quench technique. Glasses were prepared by mixing the required proportions of the reagent grade Li₂CO₃, H₃BO₃, As₂O₃ (May and Baker), MgO (Fluka) and CuO in an electrical furnace using silica crucibles. The furnace temperature is varied from 1000- 1150 °C depending on the glass composition. For samples taken from different regions of the bulk specimen, the absence of any Bragg peaks in the X-ray diffraction pattern confirmed that the glasses are amorphous and homogeneous.

The room temperature EPR spectra of powdered glass samples were recorded using a JOEL PE-3X EPR spectrometer

* e-mail: kondalou@gmail.com

operating in the X-band and employing a field modulation of 100 kHz. DPPH was used as the standard *g* marker for the determination of magnetic field. The optical absorption spectra of the present glasses in 200 – 800 nm region was recorded by using a Shimadzu spectrometer (model UV-3100) at room temperature.

3. Results and Discussion

3.1. EPR spectra

The room temperature Cu²⁺ ion doped EPR spectra of the present glasses were shown in Figure 1. The EPR spectra of Cu²⁺ ions in the remaining glasses exhibited the same spectral features. In all the EPR spectra recorded in the present investigation three parallel components were observed in the low field region. However, the perpendicular components are not resolved, leading to an intense line in the high field region.

Spectroscopic splitting (*g*) and hyperfine (*A*) tensors with axial symmetry have been assumed in the analysis of EPR spectra of oxide glasses^{20,21}. The Jahn-Teller effect causes predominantly an elongated octahedral coordination with four short in-plane bond lengths. Therefore an axial spin-Hamiltonian can be employed in the analysis of the EPR spectra which is given below:

$$H = g_{\parallel} \beta H_z S_z + g_{\perp} \beta (H_x S_x + H_y S_y) + A_{\parallel} I_z S_z + A_{\perp} (I_x S_x + I_y S_y) \quad (1)$$

where the symbols have their usual meanings²². The nuclear quadrupole contribution is neglected. The calculated spin-Hamiltonian parameters are given in Table 1.

The observed *g* values are characteristic of Cu²⁺ coordinated by six ligands, which form an octahedron elongated along the z-axis. The general nature of the ligand coordination can be obtained²³ from the fact that $g_{\parallel} g_{\perp} A_{\parallel}$ and $A_{\perp} g_{\parallel} > g_{\perp} > 2.0023$. Only an environment elongated along one of the cube axis can yield this result. In the present investigation, it is observed that $g_{\parallel} > g_{\perp} > g_c$. Therefore from the *g* values and shape of the EPR spectra, it can be concluded that the ground state of the Cu²⁺ is $d_{x^2-y^2}$ orbital, the Cu²⁺ ions being located in tetragonally distorted octahedral sites^{12,20,23,24}.

The g_{\parallel} and A_{\parallel} values are found to be dependent on the glass composition while g_{\perp} and A_{\perp} values are essentially constant. The variation of g_{\parallel} and A_{\parallel} with MgO content is illustrated in Figure 2. g_{\parallel} and A_{\parallel} varies non-linearly as the MgO content increases: g_{\parallel} decreases and then increases whereas A_{\parallel} increases and then decreases indicating the change in the tetragonal distortion of Cu²⁺ ions²⁵. The variation in g_{\parallel} and A_{\parallel} values may be associated with the change in the environment of Cu²⁺. In the B₂O₃ glasses, the addition of network modifiers (MgO and Li₂O) leads to an increase in the coordination number of a certain portion of the boron

atoms from 3 to 4. It is assumed that the resulting glass is composed of both triangular and tetrahedral units which form a relatively open network with holes between the oxygen atoms of sufficient size to accommodate the Li and Mg ions¹⁵. As a doubly charged cation, Mg²⁺ is sufficiently strong to split the network. Thus, sufficient non-bridging oxygen's are available for good coordination in the broken network. The alkali oxide Li₂O makes available additional weakly bonded O²⁻ for each Mg²⁺, i.e. Mg²⁺ captures the O²⁻ from Li₂O and this happens at the expense of Li₂O coordination. Li⁺ should remain in the neighborhood of the next stronger Mg²⁺ than that it should be incorporated separately into the rigid network. The configuration Li-O-Mg may energetically favored. The solubility of the Cu²⁺ increases with the addition of the network modifiers presumably due to the coordination of the metal ion by the extra oxygen ions. Thus, incorporation of MgO into the glass will influence the field at the site of Cu²⁺, which in turn will reflect in the non-linear variation of the spin Hamiltonian parameters as observed in the present study.

The line width of the parallel hyperfine components was found to increase with increasing values of the nuclear spin quantum number (*ml*), which may be due to fluctuations in both the ligand fields and bond covalencies from one copper (II) complex to the next, giving rise to a narrow distribution in g^{24} . The mobility of the paramagnetic species in the glass medium may also affect the EPR line shape.

3.2. Optical absorption spectra

In a regular octahedral field, the 3d⁹ configuration would result in the adegnerate ground state (²E_g). In glasses, it is assumed that no site is perfect cubic due to the disordered vitreous state. Hence, the tetragonal distortion is endemic to the vitreous state that leads to splitting of energy levels. It is observed that the elongated structures are usually more energetically favored than the compressed ones. For Cu²⁺ in an elongated octahedral symmetry, more than one band is observed¹. Figure 3 presents the optical absorption spectrum of Cu²⁺ ions in the present glasses.

The optical absorption co-efficient $\alpha(v)$, near the fundamental absorption edge of the curve in the above figure was determined from the relation

$$\alpha(v) = (1/d) \log(I_t/I_0) \quad (2)$$

where I_0 and I_t are the intensities of the incident and transmitted beams, respectively, and *d* is thickness of the glass sample. The factor $\log(I_0/I_t)$ corresponds to absorbance. Davis and Mott²⁶ and Tauc and Menth²⁷ relate this data to the optical band gap, E_{opt} through the following general relation proposed for amorphous materials

$$\alpha(v) = B(hv - E_{opt})^n / hv \quad (3)$$

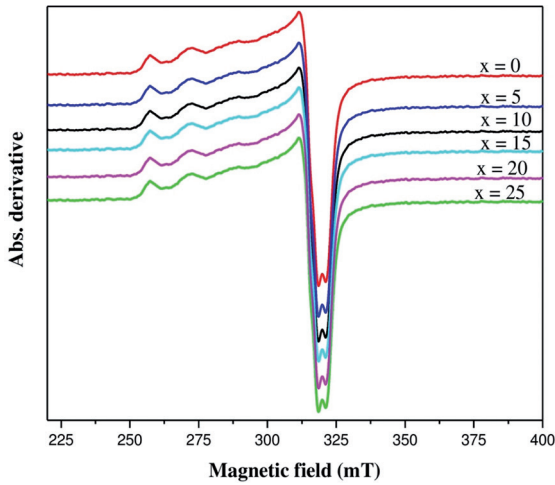


Figure 1: EPR spectra of Cu^{2+} in the present glass system.

where B is a constant related to the extent of the band tailing and $h\nu$ is incident photon energy. The index n determines the type of electronic transitions causing the absorption, and takes the values $1/2$, 2 , $3/2$ and 3 for direct allowed, indirect allowed, direct forbidden, and indirect forbidden transitions. By plotting $(\alpha h\nu)^{1/2}$ and $(\alpha h\nu)^2$ as a function of photon energy $h\nu$, one can find the optical energy band gap E_{opt} for indirect and direct transitions, respectively. The respective values of E_{opt} are obtained by extrapolating to $(\alpha h\nu)^{1/2} = 0$ for indirect transition and $(\alpha h\nu)^2 = 0$ for direct transition. Figure 4 represents the Tauc plots $\{(\alpha h\nu)^{1/2} \text{ vs } h\nu\}$ for different glass samples. The values of all optical energy gap, E_{opt} , thus obtained from the extrapolation of the linear region of Tauc plots are presented in Table 2. In the present glasses, the indirect band gap energy varies from 2.34 to 2.5 eV and direct band gap energy vary between 2.55 to 2.68 eV respectively. In the present glasses, the compositional dependence of direct and indirect optical band gap energies is illustrated in Figure 5. It is observed that the band gap

energies vary non-linearly with compositional parameter, indicating the existence of mixed alkali effect.

The main feature of the absorption edge of amorphous materials is an exponential increase of absorption coefficient $\alpha(\nu)$ with photon energy $h\nu$, which is given by the Urbach rule²⁸

$$\alpha(\nu) = C \exp(h\nu/\Delta E) \quad (4)$$

where C is a constant, and ΔE is the Urbach energy which is a measure of band tailing. The values of Urbach energy (ΔE) were determined by taking the reciprocals of slopes of the linear portion of $\ln(\alpha)$ vs $h\nu$ curves. The Urbach energy values of the present glass samples are presented in Table 2. The compositional dependence of Urbach energy ΔE is illustrated in Figure 6. Urbach energy is varying non-linearly with a compositional parameter indicating the existence of mixed alkali effect in present glasses.

The optical absorption spectra of all glasses studied reveal only a broad absorption band. The optical absorption peak position values are determined by peak pick facility of the spectrometer and are presented in Table 1 and shown in Figure 7.

The stable state of copper are Cu^+ and Cu^{2+} . The Cu^+ ion has $3d^{10}$ configuration and consequently is not expected to have any ligand field band. The Cu^{2+} ion has the $3d^9$ configuration and the spectra associated with the Cu^{2+} ion are $d-d$ transitions which can be described in terms of the ligand field theory²⁹. In a regular octahedral field, the $3d^9$ configuration would result in a degenerate ground state (2E_g) and the Jahn-Teller effect gives a marked tetragonal distortion which leads to splitting of energy levels. In glasses it is assumed that due to disordered vitreous state no site is perfectly cubic. Therefore, tetragonal distortions are endemic to the vitreous state which leads to splitting of energy levels. It is observed that the elongated structures are usually more energetically favored than the compressed

Table 1: Spin-Hamiltonian and optical absorption and bonding coefficients for Cu^{2+} ions in $x\text{MgO}-(25-x)\text{Li}_2\text{O}-50\text{B}_2\text{O}_3-25\text{As}_2\text{O}_3$ glasses.

Parameters	x=0	x=5	x=10	x=15	x=20	x=25
g_{\parallel}	2.455	2.442	2.430	2.434	2.439	2.446
g_{\perp}	2.057	2.057	2.057	2.058	2.058	2.058
A_{\parallel}	139	144	156	162	159	153
A_{\perp}	18	13	25	13	13	25
λ	722	740	758	730	769	770
G	8.276	8.038	7.819	7.751	7.840	7.966
ΔE_{xy}	12953	13513	13192	13698	13004	12987
α^2	0.901	0.906	0.928	0.970	0.964	0.933
β_1^2	0.981	0.989	0.916	0.919	0.887	0.931
β^2	0.657	0.653	0.638	0.610	0.614	0.634
Γ_{σ} (%)	21	20	16	6	18	15
Γ_{Π} (%)	4	2	17	16	23	14

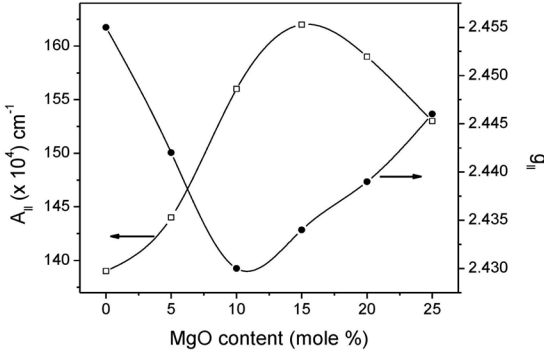


Figure 2: Variation of $g_{||}$ and $A_{||}$ with MgO content in the present study.

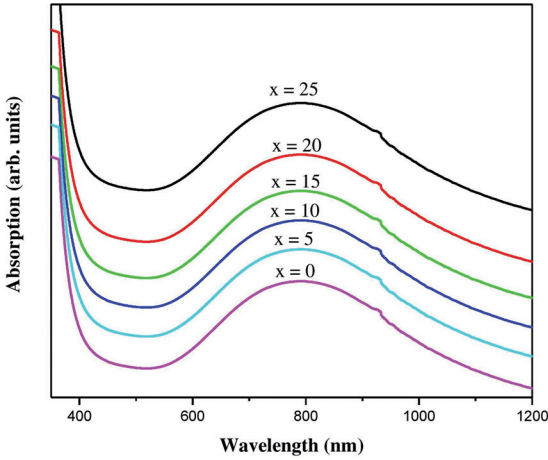


Figure 3: Optical absorption spectra of present glass system.

ones and the cupric ion exists in solution, solids and glasses in octahedral symmetry with a tetragonal distortion³⁰. For Cu²⁺ in elongated octahedral symmetry more than one band will be observed¹². But only a single optical absorption maximum was observed in most of the cases^{31,32}. This single optical band was interpreted as the overlap of all the three transitions. Hence, in the present investigation the observed asymmetric band around 13,192 cm⁻¹ is due to the overlap of ${}^2B_{1g} \rightarrow {}^2A_{1g}$ and ${}^2B_{1g} \rightarrow {}^2B_{2g}$ transitions. Most of the authors^{33,34} assigned the observed optical peak to the ${}^2B_{1g} \rightarrow {}^2B_{2g}$ transition (ΔE_{xy}) and have used this value in the evaluation of the bond parameters.

3.3. Cu²⁺ ligand bond nature

The EPR and optical absorption data can be related to evaluate the bonding coefficients of Cu²⁺. The bonding between the Cu²⁺ ion and its ligands can be described in terms of the covalency parameters α^2 , β^2 and β_1^2 where α^2 describes the in-plane σ bonding with the copper $d_{x^2-y^2}$ orbital, β^2 describes the out-of-plane π bonding with the d_{xz} and d_{yz}

orbital and the β_1^2 parameter is a measure of the in-plane π bonding with the d_{xy} orbital. The values of α^2 lie between 0.5 and 1, the limits of pure covalent and pure ionic bonding, respectively. The terms β^2 and β_1^2 can be interpreted similarly.

EPR results give rise to a new parameter (G), which is defined as

$$G = (g_{||} - g_e) / (g_{\perp} - g_e) \quad (5)$$

If the G value falls in between 3 and 5, the unit cell contains magnetically equivalent ions. If the G value is less than 3, the exchange coupling among the magnetically non-equivalent Cu(II) ions in the unit cell is not very strong. If G is greater than 5, a strong exchange coupling takes place among the magnetically non-equivalent Cu(II) ions in the unit cell. Truly compressed structures are relatively rare when compared to elongated structures³⁵.

The bonding parameters were evaluated using the equations given below³⁶

$$\alpha^2 = -(A_{||}P) + (g_{||} - 2) + 3/7(g_{\perp} - 2) + 0.04 \quad (6)$$

$$\beta_1^2 = [(g_{\perp}/g_e) - 1] \Delta E_{xy} / 3312\alpha^2 \quad (7)$$

$$\beta^2 = [(g_{\perp}/g_e) - 1] \Delta E_{xz,yz} / 828\alpha^2 \quad (8)$$

where P is the dipolar hyperfine coupling parameter. ΔE_{xy} is the energy corresponding to the transition ${}^2B_{1g} \rightarrow {}^2B_{2g}$ and λ is the spin-orbit coupling constant ($\lambda = -828$ cm⁻¹).

The corresponding value of $\Delta E_{xz,yz}$ was calculated using the approximation¹⁷

$$\Delta E_{xz,yz} = 1656K^2 / (g_{\perp}/g_e) \quad (9)$$

$$\Gamma_{\sigma} = 200(1 - S)(1 - \alpha^2) / (1 - 2S)\% \text{ and}$$

$$\Gamma_{\pi} = 200(1 - \beta_1^2)\% \quad (10)$$

where K^2 is the orbital reduction factor (= 0.77).

The normalized covalencies of Cu (II)-O in-plane bonds of σ and π symmetry are expressed³⁷ in terms of bonding coefficients α^2 and β_1^2 as follows. Where S is the overlap integral ($S_{oxy} = 0.076$). The calculated values of α^2 , β_1^2 , β^2 , are presented in Table 1. are illustrated in Figure 8. The normalized covalency of Cu (II)-O in-plane bonding of π symmetry (Γ_{π}) indicates the basicity of the oxide ion. The values of α^2 and β_1^2 indicate pure ionic for the in-plane σ bonding and in-plane π bonds, while β^2 out of the plane. Π bonding seems to be mostly covalent nature in all the glass systems.

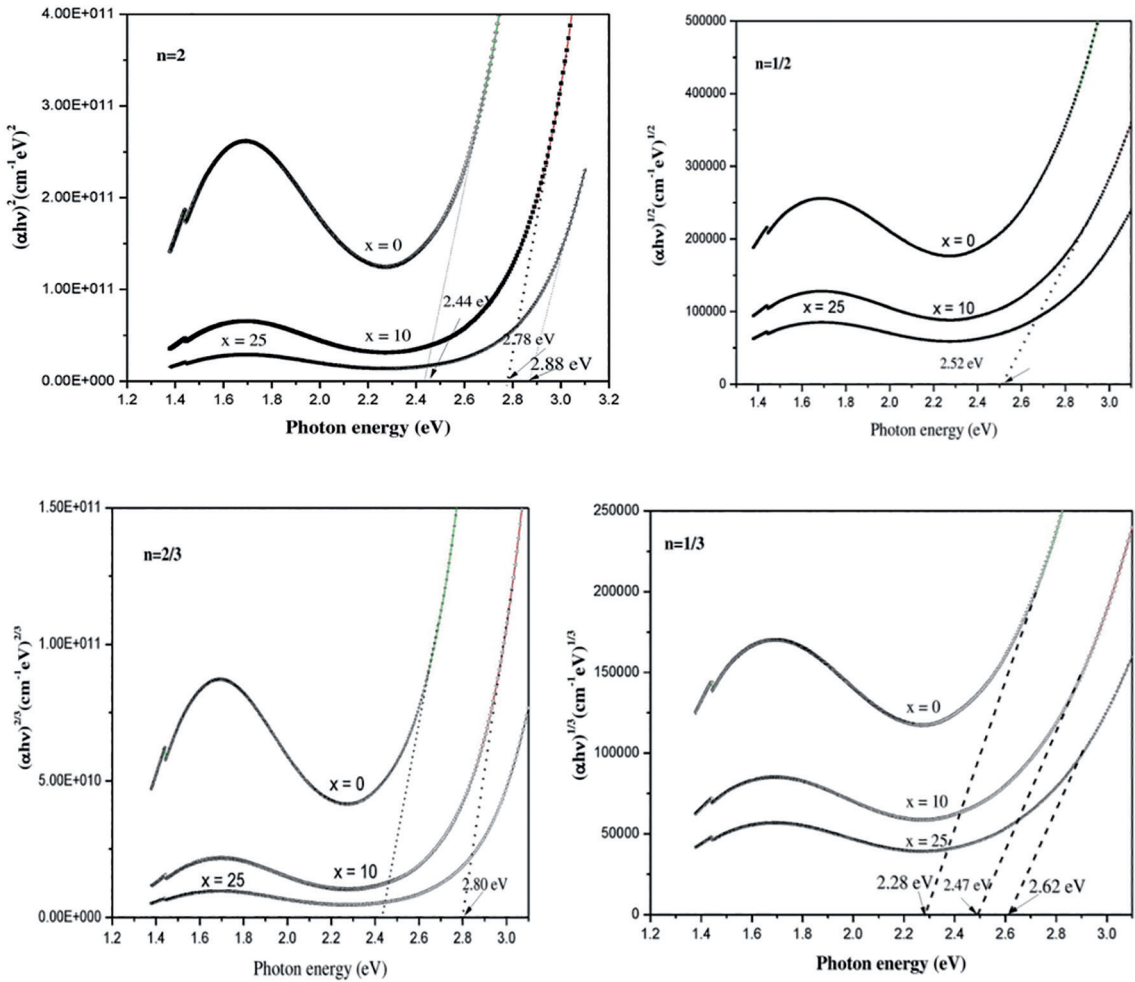


Figure 4: Tauc's plots ($n=1/2, 2, 2/3$ and $1/3$) for the present glass system.

Table 2: Optical parameters of the present glass system.

Parameter	x = 0	x = 5	x = 10	x = 15	x = 20	x = 25
Optical band gap energies (E_{opt}) (eV) (± 0.05)						
Indirect allowed ($n=1/2$)	2.50	2.39	2.42	2.34	2.38	2.41
Indirect forbidden ($n=1/3$)	2.42	3.35	2.37	3.32	2.37	2.40
Direct allowed ($n=2$)	2.66	2.59	2.68	2.62	2.55	2.64
Direct forbidden ($n=2/3$)	2.65	2.61	2.70	2.64	2.66	2.67
Urbach energy ΔE (eV) (± 0.001)	0.426	0.421	0.429	0.399	0.428	0.423

4. Conclusions

The quaternary glass system of $x\text{MgO}-(25-x)\text{Li}_2\text{O}-50\text{B}_2\text{O}_3-25\text{As}_2\text{O}_3$ ($0 \leq x \leq 25$) were prepared, and their optical and EPR measurements have been studied. The following conclusions were made: From EPR and optical measurements it is clear that Cu^{2+} ions are present in all the glasses investigated and they exist on tetragonally distorted octahedral sites with $d_{x^2-y^2}$. The spin-Hamiltonian

parameters are influenced by the composition of glass which may be attributed to the change of ligand field strength around Cu^{2+} . With increasing MgO content the ligand field strength is reduced around the Cu^{2+} ion due to the modification of the boron-oxygen network. The bond parameter values show purely ionic nature of the in-plane σ bonding and in-plane π bonding. The out-of-plane π bonding is moderately covalent.

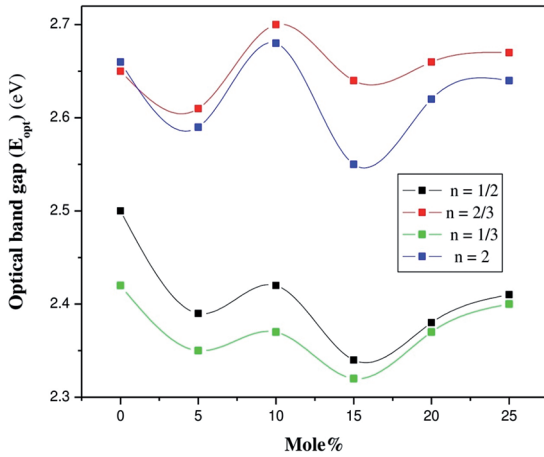


Figure 5: Optical band gap energy (for all transitions) as a function of composition (mol%) in present glasses.

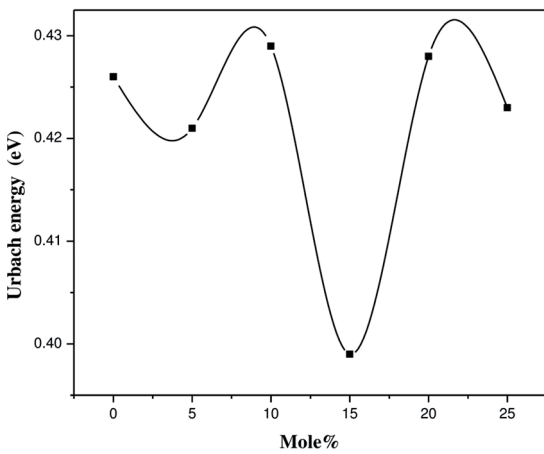


Figure 6: Compositional dependence of Urbach energy (ΔE) in the present glasses.

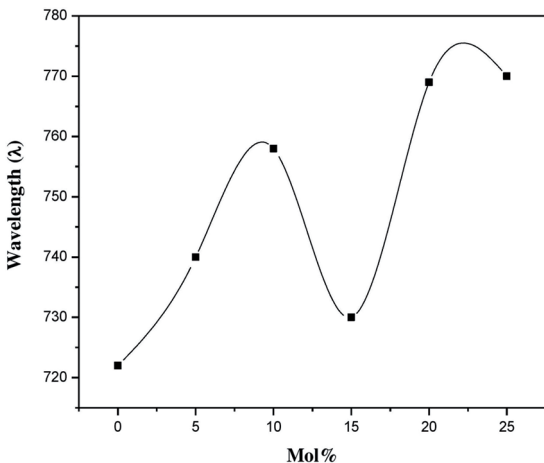


Figure 7: The compositional mole% as a function of peak position (λ).

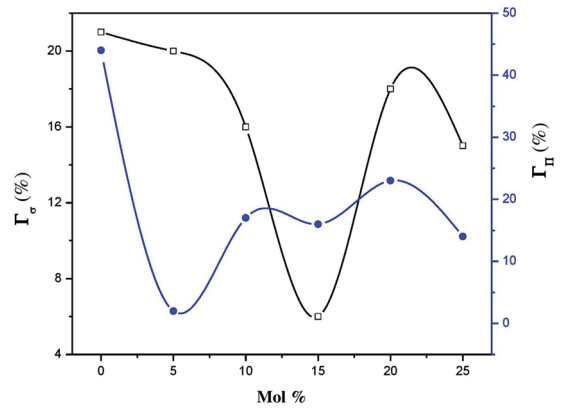


Figure 8: The mole% as a function of Γ_σ and Γ_π

5. References

- Rao NS, Bale S, Purnima M, Siva Kumar K, Rahman S. Optical absorption and electron spin resonance studies of Cu²⁺ in Li₂O–Na₂O–B₂O₃–As₂O₃ glasses. *Bulletin of Materials Science*. 2005;28(6):589-592.
- Edukondalu A, Sathe V, Rahman S, Siva Kumar K. Thermal, mechanical and Raman studies on mixed alkali borotungstate glasses. *Physica B: Condensed Matter*. 2014;438:120-126.
- Edukondalu A, Kavitha B, Samee MA, Ahmmed SK, Rahman S, Siva Kumar K. Mixed alkali tungsten borate glasses – Optical and structural properties. *Journal of Alloys and Compounds*. 2013;522:157-165.
- Ragavaiah BV, Krishna Rao D, Veeraiah N. Magnetic properties of PbO–Sb₂O₃–As₂O₃ glasses containing iron ions. *Journal of Magnetism and Magnetic Materials*. 2004;284:363-368.
- Sands RH. Paramagnetic Resonance Absorption in Glass. *Physical Review*. 1955;99(4):1222-1228.
- Castner T Jr, Newell GS, Holton WC, Slichter CP. Note on the paramagnetic resonance of iron in glass. *The Journal of Chemical Physics*. 1960;32(3):668-673.
- Kawazoe H, Hosono H, Kanazawa T. Electronic structure and properties of oxide glasses (II) Basicity measured by copper(II) ion probe in Na₂O–P₂O₅–K₂O–B₂O₃ and K₂SO₄–ZnSO₄ glasses. *Journal of Non-Crystalline Solids*. 1978;29(2):173-186.
- Shareefuddin Md, Jamal M, Narasimha Chary M. Electron spin resonance and optical absorption studies of Cu²⁺ ions in XNaI (30-X)Na₂O 70B₂O₃ glasses. *Journal of Non-Crystalline Solids*. 1996;201(1-2):95-101.
- Zhang HM, Duan JH, Xiao WB, Wan X. Theoretical studies of the local structure of Cu²⁺ center in aluminium lead borate glasses by their EPR and optical spectra. *Journal of Non-Crystalline Solids*. 2015;425:173-175.
- Klonkowski AM, Frischat GH, Richter T. The structure of sodium aluminosilicate glass. *Physics and Chemistry of Glasses*. 1983;24:166-171.

11. Rao AS, Sreedhar B, Rao JL, Lakshman SVJ. Electron paramagnetic resonance and optical absorption spectra of Mn^{2+} ion in alkali zinc borosulphate glasses. *Journal of Non-Crystalline Solids*. 1992;144:169-174.
12. Sumalatha B, Omkaram I, Rao TR, Raju CL. Alkaline earth zinc borate glasses doped with Cu^{2+} ions studied by EPR, optical and IR techniques. *Journal of Non-Crystalline Solids*. 2011;357(16-17):3143-3152.
13. Obayes HK, Wagiran H, Hussin R, Saeed MA. Structural and optical properties of strontium/copper co-doped lithium borate glass system. *Materials & Design*. 2016;94:121-131.
14. Edukondalu A, Purnima M, Srinivasy Ch, Sripathi T, Awasthi AM, Rahman S, Siva Kumar K. Mixed alkali effect in physical and optical properties of $Li_2O-Na_2O-WO_3-B_2O_3$ glasses. *Journal of Non-Crystalline Solids*. 2012;358(18-19):2581-2588.
15. Siegel I, Lorenc JA. Paramagnetic resonance of copper in amorphous and polycrystalline GeO_2 . *The Journal of Chemical Physics*. 1966;45(6):2315.
16. France PW, Carter SF, Parker JM. Oxidation states of 3d transition metals in ZrF_4 glasses. *Physics and Chemistry of Glasses*. 1986;27:32-41.
17. Hetch HG, Johnston TS. Study of the structure of vanadium in soda-boric oxide glasses. *The Journal of Chemical Physics*. 1967;46(1):23-29.
18. Dietzel AH. On the so-called mixed alkali effect. *Physics and Chemistry of Glasses*. 1983;24:172-180.
19. Ramdevudu G, Shareefuddin Md, Bai NS, Rao ML, Chary MN. Electron paramagnetic resonance and optical absorption studies of Cu^{2+} spin probe in $MgO-Na_2O-B_2O_3$ ternary glasses. *Journal of Non-Crystalline Solids*. 2000;278(1-3):205-212.
20. Day DE. Mixed alkali glasses – their properties and uses. *Journal of Non-Crystalline Solids*. 1976;21(3):343-372.
21. Ragavaiah BV, Laxmikanth C, Veeriah N. Spectroscopic studies of titanium ions in $PbO-Sb_2O_3-As_2O_3$ glass system. *Optics Communications*. 2004;235(4-6):341-349.
22. Rao NS, Bale S, Purnima M, Siva Kumar K, Rahman S. Mixed alkali effect in boroarsenate glasses. *Journal of Physics and Chemistry of Solids*. 2007;68(7):1354-1358.
23. Bleaney B, Bowers KD, Ingram DJE. Paramagnetic Resonance in Diluted Copper Salts. I. Hyperfine Structure in Diluted Copper Tutton Salts. *Proceedings of Royal Society: A*. 1955;228:147-157.
24. Imagawa H. ESR Studies of Cupric Ion in Various Oxide Glasses. *Physica Status Solidi B*. 1968;30(2):469-478.
25. Ohishi Y, Mitachi S, Kanamori T, Manabe T. Optical absorption of 3d transition metal and rare earth elements in zirconium fluoride glasses. *Physics and Chemistry of Glasses*. 1983;24(5):135-140.
26. Davis EA, Mott NF. Conduction in non-crystalline systems V. Conductivity, optical absorption and photo conductivity in amorphous semiconductors. *Philosophical Magazine*. 1970;22(179):903-922.
27. Tauc J, Mentel A. States in the gap. *Journal of Non-Crystalline Solids*. 1972;8-10:569-585.
28. Urbach F. The long wavelength edge of photographic sensitivity and of the electronic absorption of solids. *Physical Review*. 1953;92:1324.
29. Bandyopadhyay AK. Optical and ESR investigation of borate glasses containing single and mixed transition metal oxides. *Journal of Materials Science*. 1981;16(1):189-203.
30. Bates T, Mackenzie JD. Ligand Field Theory and Absorption Spectra of Transition Metal Ions in Glasses. In: Mackenzie JD, ed. *Modern Aspects of the Vitreous State*. Vol 2. London: Butterworths; 1962. p. 195-254.
31. Jorgensen CK. Comparative crystal field studies of some ligands and the lowest single state of paramagnetic nickel(II) complexes. *Acta Chemica Scandinavica*. 1955;9:1362-1377.
32. Orgel LE. Band Widths in the Spectra of Manganous and Other Transition-Metal Complexes. *The Journal of Chemical Physics*. 1955;23(10):1824-1826.
33. Ballhausen CJ. *Introduction to Ligand Field Theory*. New York: McGraw-Hill; 1962.
34. Maki AH, Mc Garvey BR. Electron Spin Resonance in Transition Metal Chelates. I. Copper (II) Bis-Acetylacetonate. *The Journal of Chemical Physics*. 1958;29(1):31-38.
35. Reddy SL, Endo T, Siva Reddy G. Electronic (absorption) spectra of 3d transition metal complexes. In: Farrukh MA, ed. *Advanced Aspects of Spectroscopy*. Rijeka: Intech; 2012. p. 1-48.
36. Kivelson D, Neiman R. ESR studies on the bonding in copper complexes. *The Journal of Chemical Physics*. 1961;35(1):149-155.
37. van Veen G. Simulation and analysis of EPR spectra of paramagnetic ions in powders. *Journal of Magnetic Resonance (1969)*. 1978;30(1):91-109.